ISSN 1674-1056
http://cpb.iphy.ac.cn
http://iopscience.iop.org/cpb
中国物理 B
Chinese Physics
中国物理
Chinese Physics B

Effect of metal fluorides on chromium ions doped bismuth borate glasses for optical applications

L Haritha, K Chandra Sekhar, R Nagaraju, G Ramadevudu, Vasanth G Sathe, Md. Shareefuddin

Citation: Chin. Phys. B . 2019, 28(3): 038101. **doi:** 10.1088/1674-1056/28/3/038101
Journal homepage: http://cpb.iphy.ac.cn; http://iopscience.iop.org/cpb

What follows is a list of articles you may be interested in

LaGa-based bulk metallic glasses

Lin-Zhi Zhao(赵林志), Rong-Jie Xue(薛荣洁), Wei-Hua Wang(汪卫华), Hai-Yang Bai(白海洋)
Chin. Phys. B . 2017, 26(1): 018106. **doi:** 10.1088/1674-1056/26/1/018106

Amorphous phase formation rules in high-entropy alloys

Qiu-Wei Xing(邢秋玮), Yong Zhang(张勇)
Chin. Phys. B . 2017, 26(1): 018104. **doi:** 10.1088/1674-1056/26/1/018104

Generalized model for laser-induced surface structure in metallic glass

Lin-Mao Ye(叶林茂), Zhen-Wei Wu(武振伟), Kai-Xin Liu(刘凯欣), Xiu-Zhang Tang(汤秀章), Xiang-Ming Xiong (熊向明)
Chin. Phys. B . 2016, 25(6): 068104. **doi:** 10.1088/1674-1056/25/6/068104

Raman scattering study of phase transition in Lu_2O_3-Ta_2O_5

Wang Xiao-Fei, Xing Xue, Zhang Qing-Li, You Jing-Lin, Wu Jun, Zhang De-Ming, Sun Yu, Sun Dun-Lu, Yin Shao-Tang
Chin. Phys. B . 2015, 24(9): 098104. **doi:** 10.1088/1674-1056/24/9/098104

Epitaxial growth of $Ge_{1-x}Sn_x$ films with x up to 0.14 grown on Ge (00l) at low temperature

Tao Ping, Huang Lei, Cheng H H, Wang Huan-Hua, Wu Xiao-Shan
Chin. Phys. B . 2014, 23(8): 088112. **doi:** 10.1088/1674-1056/23/8/088112

Effect of metal fluorides on chromium ions doped bismuth borate glasses for optical applications

L Haritha[1], K Chandra Sekhar[2,†], R Nagaraju[3], G Ramadevudu[3], Vasanth G Sathe[4], and Md. Shareefuddin[2]

[1] *Department of Physics, Telangana University, Nizamabad, Telangana* 503322, *India*
[2] *Department of Physics, Osmania University, Hyderabad, Telangana* 500007, *India*
[3] *Department of Physics, Vasavi College of Engineering, Hyderabad, Telangana* 500031, *India*
[4] *UGC-DAE Consortium of Scientific Research, Indore* 452017, *India*

(Received 13 September 2018; revised manuscript received 29 November 2018; published online 25 February 2019)

Fluoride based glasses with composition CaF_2–ZnF_2–Bi_2O_3–B_2O_3 doped with chromium ions have been investigated using physical, optical, electron paramagnetic resonance (EPR), Fourier-transform infrared spectroscopy (FTIR), and Raman studies. The amorphous nature of samples was confirmed from x-ray diffraction spectra. The density is evaluated from the Archimedes principle and the values of optical band gap and Urbach energy values were evaluated from the optical absorption spectra. Thus, molar volume, refractive index, etc., were also evaluated. The observed decrease in density and the optical band gap with CaF_2 is explained using the crystalline density of metal fluorides and the ionicity of fluorine ions, respectively. The three peaks near 450 nm, 606 nm, and 720 nm, which are shown in the absorption spectra, are accredited to $^4A_{2g} \rightarrow {}^4T_{1g}$, $^4A_{2g} \rightarrow {}^4T_{2g}$, $^4A_{2g} \rightarrow {}^2E$ transitions, respectively. Resonance signals at $g \approx 4.82$ and $g \approx 1.99$ were observed in EPR spectra which are assigned. FTIR and Raman analysis were carried out to examine the impact of metal fluorides on the structure of bismuth borate glasses.

Keywords: glasses, x-ray diffraction, electron paramagnetic resonance, Fourier-transform infrared spectroscopy (FTIR), Raman spectra

PACS: 81.05.Kf, 76.30.–v, 78.30.–j **DOI:** 10.1088/1674-1056/28/3/038101

1. Introduction

In recent decades, there has been a huge demand for optically transparent materials which have applications in the fields of telecommunication and optoelectronic devices. The literature survey suggested that the oxide-based glasses such as tellurite, phosphate, silicate, and borates were widely studied. Our interest in borate glasses is due to its low cost, low melting temperature, wide range of composition, glass forming ability with most of the elements besides its promising applications.[1–5] In contrast to the oxide-based glasses, fluoride glasses have many advantages such as wide transmission window, low phonon energy, low OH contents, large solubility for rare-earth ions, wide transmission range, and long fluorescence lifetime.[6–11]

From the literature it is evident that pure Bi_2O_3 glass cannot be obtained. However, the addition of small amounts of conventional glass formers (B_2O_3, P_2O_5, etc) with a larger addition of Bi_2O_3, can lead to the glass formation. Bismuth borate glasses have received more attention due to their special properties as photo induced nonlinear optical materials.[12–18]

Fluoroborates, are the main class of borates which have been extensively used in many diversified fields such as flame retardants, optic materials, and textiles. The properties of these fluoroborates can be improved by the addition of metals like zinc, sodium, etc. Zinc fluoroborate and other additives compose fire-retardant finishing compositions, especially useful for synthetic fibers. Hence, it is worthwhile to look at the properties of the combination of calcium and zinc.[19–26] Moreover, in the recent past, several researchers have been motivated towards doped transition metal ion glasses due to their interesting applications like memory devices, radiation sensitive materials, solid state laser, etc. In the literature, transition metal ions like Cr^{3+}, Ni^{2+}, VO^{2+}, and Cu^{2+} have been widely studied.[27–30] Amongst all doped transition metal glasses, the Cr^{3+} ion-doped glasses are given importance as they have applications in tunable solid state lasers, fiber optical communication, etc.[31–34]

Keeping in view the role of chromium in the glass matrices and the importance of bismuth borate glasses, authors have investigated the physical and spectroscopic studies of CaF_2–ZnF_2–Bi_2O_3–B_2O_3 glasses doped with chromium ions.

2. Experimental

2.1. Sample preparation

In the present investigation, glass samples of the desired composition xCaF$_2$–$(20-x)$ZnF$_2$–20Bi$_2$O$_3$–59.8B$_2$O$_3$–0.2Cr$_2$O$_3$ ($0 \leq x \leq 20$ mole%) were prepared by the classical melt-quenching technique. Analar grade chemicals CaF_2 (Himedia), ZnF_2 (Himedia), Bi_2O_3 (Sigma-Aldrich), H_3BO_3 (Sigma-Aldrich), and Cr_2O_3 (Sigma-Aldrich) were used in

†Corresponding author. E-mail: chandu9417@gmail.com

© 2019 Chinese Physical Society and IOP Publishing Ltd

preparation. These starting materials were taken in proportions and mixed homogeneously in an agate mortar with a pestle. These mixtures were melted in porcelain crucibles at 1173 K in an electrical furnace for 45 min. To attain better homogeneity, the mixture was stirred periodically. The bubble-free transparent melt was poured onto a pre-heated stainless steel (SS) plate and subsequently pressed by the other SS plate to obtain glass samples. The glass compositions are given in Table 1.

Table 1. Compositions of xCaF$_2$–$(20-x)$ZnF$_2$–20Bi$_2$O$_3$–59.8B$_2$O$_3$–0.2Cr$_2$O$_3$ ($0 \le x \le 20$ mole%) glass samples in mole%.

Glass code	CaF_2	ZnF_2	Bi_2O_3	B_2O_3	Cr_2O_3
CZBBCR1	0	20	20	59.8	0.2
CZBBCR2	5	15	20	59.8	0.2
CZBBCR3	10	10	20	59.8	0.2
CZBBCR4	15	5	20	59.8	0.2
CZBBCR5	20	0	20	59.8	0.2

2.2. Sample characterization

A Philips Xpert PRO XRD (Pan Analytical) model was used for recording XRD spectra. The 2θ values were recorded over the range from 10° to 80°. Density (ρ) measurements were carried on CZBBCR glasses using Archimedes principle in which xylene ($\rho_b = 0.865$ gm/cc) is used as the immersion liquid. For each glass composition, a minimum of three samples were used to estimate the density. A random error in the measurement of density values was about ±1%. The JASCO V-760 UV–visible spectrophotometer, built with a double beam monochromator for obtaining high resolution, is used for recording optical absorption spectra of the polished samples in absorption mode at room temperature (RT). Electron paramagnetic resonance (EPR) spectra of the samples were recorded at RT using (BRUKER) EPR spectrometer at frequency (9.7 GHz) with a modulating frequency of 100 kHz. The errors in 'g' and 'A' values are about ±0.002 and $\pm 2 \times 10^{-4}$ cm^{-1}, respectively. The FTIR spectrum of the samples is scanned in the range 400–1600 cm^{-1} on JASCO-FTIR-4600 spectrophotometer with an accuracy of ±0.01 cm^{-1} and resolution of 0.7 cm^{-1} at RT. A KBr pellet technique was used, 1:100 ratios of powdered glass sample and KBr are mixed and obtained in the form of a pellet under an applied load. The sample in pellet form is used for recording the FTIR spectrum of the glasses. The Raman measurements were performed on CZBBCR glasses in the range 200–1600 cm^{-1} on a Jobin–Yvon Horiba (LABRAM HR-800) system inbuilt with high stable confocal microscope for micro Raman 10x, 50x, 100x objective lens. A suitable objective lens can be taken to focus the laser onto the spot from ~ 1–5 micron.

3. Results and discussion

3.1. X-ray diffraction

X-ray diffraction studies of the samples confirm the crystalline structure with sharp Braggs characteristics peaks. The sharp peaks are due to long range orderliness in the materials. The absence of such sharp peaks indicates the short range order. Particularly in glassy materials only short range order is prevailing and shows no sharp peaks. X-ray diffraction patterns of CZBBCR glasses have shown broad humps over the range from 10° to 80° of 2θ values as indicated in Fig. 1. The absence of Bragg peaks in the spectra did not show any crystalline nature.

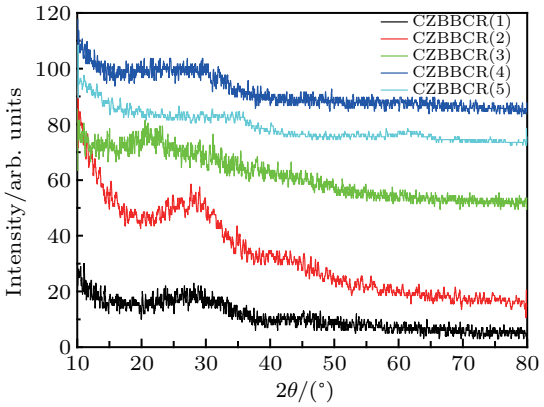


Fig. 1. XRD spectra of xCaF$_2$–$(20-x)$ZnF$_2$–20Bi$_2$O$_3$–59.8B$_2$O$_3$–0.2Cr$_2$O$_3$ ($0 \le x \le 20$ mole%) glass samples.

3.2. Density and Molar volume

Density (ρ) is the primary physical property of any solid material, which prospects the strength and structural changes in any material. Its variation depends on many physical quantities like coordination number, compactness, etc. Density plays an important role in understanding the modification of BO_3 into four fold BO_4 units, and *vice versa*.[1,34–36] In the present study, it was found that the density decreases from 5.236 gm/cc (CZBBCR1) to 4.819 gm/cc (CZBBCR5) with increasing CaF_2 concentration. The molar volume (V_m) was estimated from density and the molecular weight (M) of the glass sample. Figure 2 shows the response of ρ and V_m with CaF_2.

From previous literature, the variation in density is explained using the physical parameters like crystal density, molecular weight and/or ionic radius.[1,34,37–39] The gradual enhancement in the mole percentage of CaF_2 in the CZBBCR glass system caused a nonlinear decrease in the density, which is suitably explained using the crystal density of calcium fluoride (3.18 gm/cc) which is lesser than zinc fluoride (4.95 gm/cc). It can also be assigned to fractional replacement of low molecular weight CaF_2 (78.07 g/mol) by the high molecular weight ZnF_2 (103.406 g/mol). The decrease in density may be due to the conversion of [BO_4] into [BO_3] units.

It was reported that the [BO_4] structural units are denser than [BO_3] structural units, hence decrease in strong connectivity in the glass network results in an increase in the inter-atomic spacing and forms less compact glass.

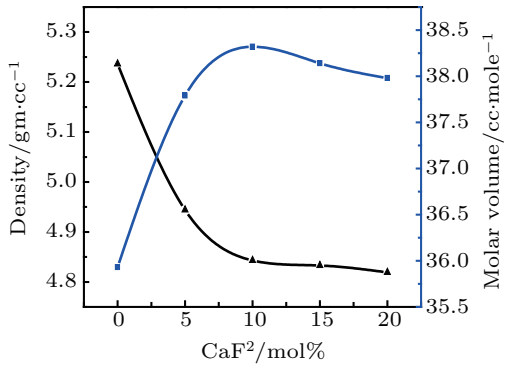


Fig. 2. Variation of density and molar volume with CaF_2 in $x$$CaF_2$–$(20-x)$$ZnF_2$–$20Bi_2O_3$–$59.8B_2O_3$–$0.2Cr_2O_3$ ($0 \le x \le 20$ mole%) glass samples.

3.3. Optical absorption

Figure 3 shows optical absorption spectra of CZBBCR glass samples. All the spectra have shown characteristic peaks at around 440 nm, 610 nm, and 680 nm, and are ascribed to $^4A_{2g} \rightarrow {}^4T_{1g}$, $^4A_{2g} \rightarrow {}^4T_{2g}$, $^4A_{2g} \rightarrow {}^2E$ transitions, respectively. Crystal field and Rachah parameters (D_q, B, and C) have been calculated using these transitions and the following relations and presented in Table 3.[34,40–43]

$$D_q = \frac{1}{10}[E(^4A_{2g} \rightarrow {}^4T_{2g})], \tag{1}$$

$$\frac{B}{D_q} = \frac{(\frac{\Delta E}{D_q})^2 - 10(\frac{\Delta E}{D_q})}{15(\frac{\Delta E}{D_q} - 8)}, \tag{2}$$

$$\frac{E(2_E)}{B} \cong 3.05\frac{C}{B} + 7.90 + 1.80\frac{D}{D_q}. \tag{3}$$

In the present investigation of CZBBCR glass samples, the B value is 515 cm^{-1} for CZBBCR1, 625 cm^{-1} for CZBBCR2, 575 cm^{-1} for CZBBCR3, 565 cm^{-1} for CZBBCR4, and 694 cm^{-1} for CZBBCR5 glass sample. It can be seen that the obtained B values for all CZBBCR glass samples are far less than the free-ion B value 1030 cm^{-1}. The lesser value of B suggests that the d-shell electrons are shielded by boron network in CZBBCR glasses. D_q/B value estimates the strength of the crystal field. It is well known that from earlier work, for weak crystal field $D_q/B \ll 2.3$, for strong fields $D_q/B \gg 2.3$, and for intermediate crystal fields D_q/B is 2.3.[44] In the present glass system, the D_q/B values for all the samples are greater than 2.3, which suggests that the Cr^{3+} ions are in the strong crystal field.

Figure 4 shows the Tauc plots of CZBBCR glass samples. Optical band gap values were evaluated using Davis and Mott[45] and Tauc and Menth[46] relation for indirect optical transitions.

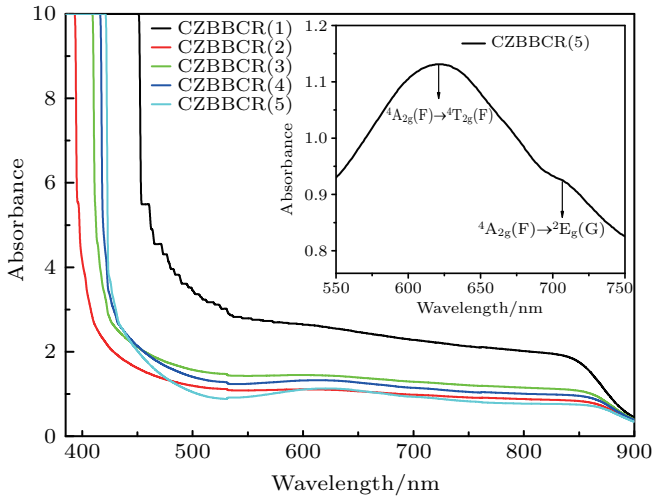


Fig. 3. Optical absorption spectra of $x$$CaF_2$–$(20-x)$$ZnF_2$–$20Bi_2O_3$–$59.8B_2O_3$–$0.2Cr_2O_3$ ($0 \le x \le 20$ mole%) glass samples. Inset: absorption spectra of CZBBCR5 sample with peak positions.

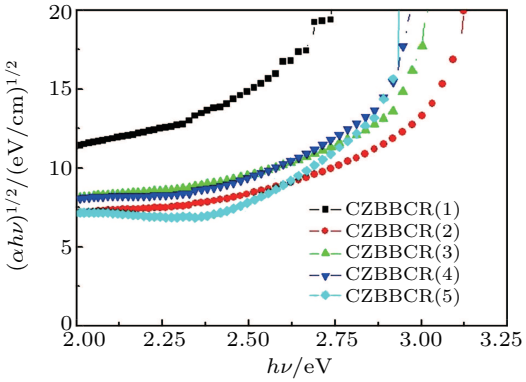


Fig. 4. Tauc plots of $x$$CaF_2$–$(20-x)$$ZnF_2$–$20Bi_2O_3$–$59.8B_2O_3$–$0.2Cr_2O_3$ ($0 \le x \le 20$ mole%) glass samples.

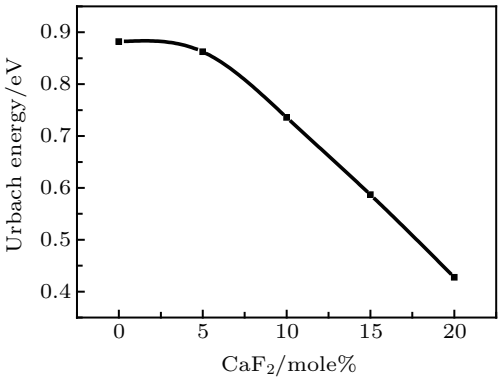


Fig. 5. Variation of Urbach energy with CaF_2 in $x$$CaF_2$–$(20-x)$$ZnF_2$–$20Bi_2O_3$–$59.8B_2O_3$–$0.2Cr_2O_3$ ($0 \le x \le 20$ mole%) glass samples.

The optical band gap value for CaF_2 free sample (CZBBCR1) is 2.143 eV, whereas for CZBBCR2 the band gap is 2.691 eV and seems to decrease with the increase in composition of CaF_2. Only for the 5 mol% addition of CaF_2 to the glass network, the band gap is enhanced. Further, the gradual increase of CaF_2 (replacement of ZnF_2 with CaF_2, i.e., Zn^{2+} with Ca^{2+}) decreases the band gap value. As electronegativity of Zn^{2+} (1.65) is greater than Ca^{2+} (1.00), ionicity of fluorine

ions increases with the increase of CaF_2 and hence band gap values decrease from CZBBCR2 to CZBBCR4.

Figure 5 shows the variation of Urbach energy (ΔE) with CaF_2 mole%. The ΔE values vary from 0.882 eV (CZBBCR1) to 0.4276 eV (CZBBCR5). The materials with larger ΔE values are believed to have a greater tendency to convert weak bond into defects.[47,48] The obtained values of ΔE for the present glass system decrease nonlinearly with the increase of CaF_2, suggesting an increase of more orderliness.

The refractive index (n), molar refraction (R_m), and molar polarizibility (α_m) values of the CZBBCR samples are evaluated from the following relations:[49,50]

$$\frac{n^2-1}{n^2+2} = 1 - \sqrt{\frac{E_{opt}}{20}}, \tag{4}$$

$$R_m = \frac{n^2-1}{n^2+2} V_m, \tag{5}$$

$$\alpha_m = \left(\frac{3}{4\Pi N_A}\right) R_m. \tag{6}$$

The values of n, R_m, and α_m are given in Table 2. Variation of 'n' values shows the behavior opposite to optical band gaps and the values vary between 2.486 and 2.677. The high value of index of refraction of CZBBCR glass system finds the applications in optical fiber communication.

Table 2. Molecular weight (M), density (ρ, gm/cc), molar volume (V_m, cc/mole), Urbach energy (ΔE, eV), optical band gap (E_{opt}, eV), refractive indexes (n), molar refraction (R_m, cc/mole), and molar electronic polarizability (α_m, cc/mole) of xCaF$_2$–$(20-x)$ZnF$_2$–20Bi$_2$O$_3$–59.8B$_2$O$_3$–0.2Cr$_2$O$_3$ ($5 \le x \le 20$ mole%) glass samples.

Glass code	M	ρ	V_m	ΔE	E_g	n	R_m	$\alpha_m/10^{-24}$
CZBBCR1	188.12	5.236	35.93	0.882	2.143	2.677	24.15	9.26
CZBBCR2	186.86	4.944	37.79	0.7359	2.691	2.486	23.93	9.18
CZBBCR3	185.59	4.843	38.32	0.8624	2.651	2.498	24.37	9.34
CZBBCR4	184.32	4.833	38.14	0.5867	2.615	2.509	24.35	9.33
CZBBCR5	183.06	4.819	37.98	0.4276	2.544	2.532	24.43	9.36

3.4. Electron paramagnetic resonance (EPR)

The theory of EPR spectra related to chromium ions was reported by many researchers.[30,34,37,51,52] Figure 6 shows the EPR spectra of xCaF$_2$–$(20-x)$ZnF$_2$–20Bi$_2$O$_3$–59.8B$_2$O$_3$–0.2Cr$_2$O$_3$ (x = 0, 5, 10, 15, and 20 mole%) glass samples. EPR spectra exhibited an intense resonance signal centered at $g \approx 4.3$ and $g \approx 1.97$. The g values varied from 4.265 to 4.316 and 1.988 to 1.993 for low field and high field portion, respectively. According to the Landry theory, the spectrum on the lower field side ($g \approx 4.3$) is from the isolated ions of chromium, whereas the high field side ($g \approx 1.99$) is due to exchange coupled pairs Cr^{3+}–Cr^{3+}.[53–55]

Noticeable change in g values is not observed, but nonlinear reduction in the intensity of the EPR spectra at $g \approx 2.0$, i.e., in the high field region, has been noticed as we move from CZBBCR1 to CZBBCR5 glass sample. Hence, on increasing CaF_2 concentration, interaction of the exchange coupled pairs of chromium ions decreases.

The number of spins (N) participating in the resonance and the magnetic susceptibility (χ) were calculated and are given in Table 4.[56,57] The N value for CZZBBCR glasses decreases nonlinearly from CZBBCR1 to CZBBCR5, which is attributed to the decrease in the intensity of EPR signal. The χ values vary proportionally with N.

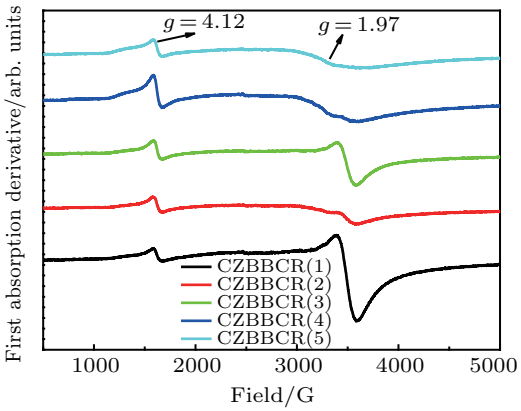


Fig. 6. EPR spectra of xCaF$_2$–$(20-x)$ZnF$_2$–20Bi$_2$O$_3$–59.8B$_2$O$_3$–0.2Cr$_2$O$_3$ ($0 \le x \le 20$ mole%) glass samples.

Table 3. Absorption peak positions, corresponding transitions and Racah parameters (D_q/B, B, and C) for xCaF$_2$–$(20-x)$ZnF$_2$–20Bi$_2$O$_3$–59.8B$_2$O$_3$–0.2Cr$_2$O$_3$ ($0 \le x \le 20$ mole%) glass samples.

Glass code	$^4A_{2g} \rightarrow {}^4T_{1g}$		$^4A_{2g} \rightarrow {}^4T_{2g}$		$^4A_{2g} \rightarrow {}^2E$		D_q	B	D_q/B	C
	λ/nm	cm^{-1}	λ/nm	cm^{-1}	λ/nm	cm^{-1}				
CZBBCR1	456	21929	606	16501	720	13888	1650.1	515	3.200	3314
CZBBCR2	439	22779	608	16447	725	13793	1644.7	625	2.629	3043
CZBBCR3	442	22624	600	16666	728	13736	1666.6	575	2.895	3131
CZBBCR4	449	22271	609	16420	714	14005	1642.0	565	2.905	3243
CZBBCR5	436	22935	620	16129	718	13927	1612.9	694	2.325	2944

Table 4. g-value, number of spins (N), and magnetic susceptibility (χ) of xCaF$_2$–$(20-x)$ZnF$_2$–20Bi$_2$O$_3$–59.8B$_2$O$_3$–0.2Cr$_2$O$_3$ ($0 \leq x \leq 20$ mole%) glass samples.

Glass code	g (low field side)	g (high field side)	$N(10^{22})$ per Kg	$\chi/10^{-3}$ m^3/Kg
CZBBCR1	4.265	1.992	5.22	12.54
CZBBCR2	4.316	1.988	5.16	12.34
CZBBCR3	4.301	1.993	4.54	10.92
CZBBCR4	4.310	1.990	3.61	8.65
CZBBCR5	4.274	1.992	2.08	4.99

3.5. FTIR spectra

Structural details of glasses can be gathered from the FT–IR spectroscopy. Figure 7 shows the FT–IR spectra of CZBBCR glass samples. Generally, IR spectra of borate glasses are mainly classified into three regions. The bands in the region i) 1600–1200 cm^{-1} are due to BO_3 units, ii) 1200 and 800 cm^{-1} belongs to BO_4 units; and iii) $\sim$ 700 cm^{-1} corresponds to the B–O–B bending vibrations.[58–60] The band positions and assignments are listed in Table 5. The band positioned at 450 cm^{-1} is due to the metal cation (Zn^{2+} and Ca^{2+}) vibrations. The bands around 540 cm^{-1} are attributed to the vibrations of Bi–O bonds in BiO_6 units. The wave numbers from 672–720 cm^{-1} are attributed to bending vibration of B–O–B in [BO_3] triangles and the symmetric stretching vibrations of Bi–O bonds in BiO_3 pyramidal units and stretching vibrations of B–O–B bonds in BO_3 unit groups.[18,61,62] The second one, 867–1052 cm^{-1}, is attributed to B–O stretching vibration of BO_4 units which were shared by various borate groups, like penta-borate, tri-borate, and di-borate groups. Band at 880 cm^{-1} may be attributed to the B–O stretch in BO borate groups and/or ascribed to the symmetrical stretching vibrations of Bi–O bonds of [BiO_3] units.[18,62,63] Another band $\sim$ 960 cm^{-1} is attributed to the B–O stretch in BO_4 units from diborate groups. The stretching vibrations of B–O–B in the [BO_4] tetrahedron are found in the wavenumber range from 1052 to 1038 cm^{-1}. The deep band at 1250 cm^{-1} is caused due to the B–O stretching vibration of trigonal BO_3 units from meta and ortho-borate group. Stretching vibrations of B–O bond from ortho-borate groups are due to the band at 1213–1246 cm^{-1}. The band at 1370 cm^{-1} is the stretching vibration of B–O–B in [BO_3] triangles. The bands between 1174–1266 cm^{-1} arise due to stretching of BO_3 units from pyro- and ortho-borate groups and 1320–1435 cm^{-1} arise due to the asymmetric stretching of the B–O bonds in BO_3 units.[1,18,64–67]

Table 5. FTIR band assignments of xCaF$_2$–$(20-x)$ZnF$_2$–20Bi$_2$O$_3$–59.8B$_2$O$_3$–0.2Cr$_2$O$_3$ ($0 \leq x \leq 20$ mole%) glass samples.

Wavenumber/cm^{-1}	Band assignments
$\sim$ 450	Metal cation (Zn^{2+} and Ca^{2+}) vibrations
$\sim$ 545	Vibrations Bi–O bonds in BiO_6 units
$\sim$ 720	Bending vibration of B–O–B in [BO_3] triangles and stretching vibrations of B–O–B bonds in BO_3 units groups
$\sim$ 874	B–O stretch in BO borate groups
$\sim$ 962	B–O stretch in BO_4 units from diborate groups
$\sim$ 1038	Stretching vibrations of B–O–B in [BO_4] tetrahedron
$\sim$ 1256	Stretching vibration of trigonal BO_3 units from meta and ortho-borate group
1356–1452	Asymmetric stretching of B–O bonds in BO_3 units

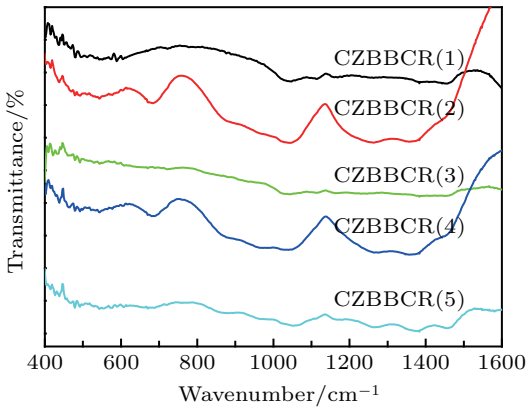


Fig. 7. FTIR spectra of xCaF$_2$–$(20-x)$ZnF$_2$–20Bi$_2$O$_3$–59.8B$_2$O$_3$–0.2Cr$_2$O$_3$ ($0 \leq x \leq 20$ mole%) glass samples.

3.6. Raman spectra

Raman spectra of CZBBCR glass samples are shown in Fig. 8 and deconvoluted spectrum of CZBBCR2 is shown in Fig. 9. Raman spectra are spread over in the region from 200 cm^{-1} to 1600 cm^{-1}. The Raman bands found at $\sim$ 133, $\sim$ 278, $\sim$ 368, $\sim$ 451, $\sim$ 580, $\sim$ 683, $\sim$ 863, $\sim$ 1258, $\sim$ 1326, and $\sim$ 1400 cm^{-1} (Table 6). It has been observed that the vibrations arising from Bi_2O_3 groups fall at lower numbers as compared to the vibrations of B_2O_3. The peak centered at 133 cm^{-1} indicates the presence of the Bi^{3+} in [BiO_6] units, which supports that the bismuth has network forming nature, while the bands between 270–580 cm^{-1} are due to the sym-

metric stretching anion motion in angular-regulated cation–anion–cation configurations in [BiO_6] polyhedral.[67,68] The band at 680 cm^{-1} is due to the stretching of B–O- bonds connected to borate groups. The bands at ~ 860 and ~ 1250 cm^{-1} are due to symmetric stretching vibrations of B–O–B bridges and pyroborate groups, respectively. The band at ~ 1330 cm^{-1} is due to $B\O_2O^-$ triangles linked to $B\O_4^-$ units. The band at ~ 1400 cm^{-1} is assigned to the stretching of B–O bands attached to the borate groups.[69–71]

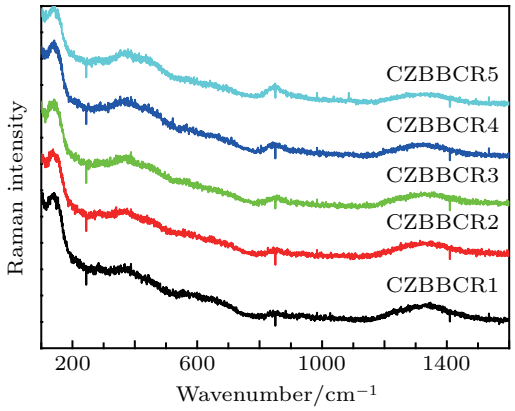


Fig. 8. Raman spectra of $x$$CaF_2$–$(20-x)$$ZnF_2$–$20Bi_2O_3$–$59.8B_2O_3$–$0.2Cr_2O_3$ ($0 \le x \le 20$ mole%) glass samples.

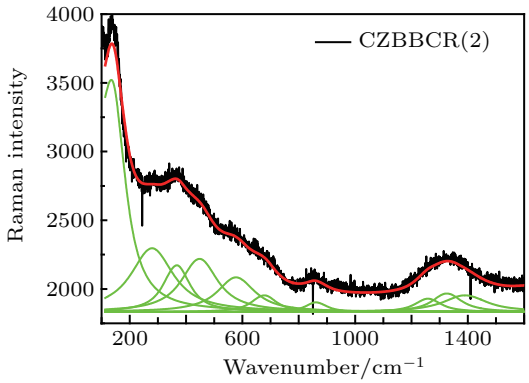


Fig. 9. Deconvoluted Raman spectra of $5CaF_2$–$15ZnF_2$–$20Bi_2O_3$–$59.8B_2O_3$–$0.2Cr_2O_3$ glass sample.

Table 6. Raman band assignments of $x$$CaF_2$–$(20-x)$$ZnF_2$–$20Bi_2O_3$–$59.8B_2O_3$–$0.2Cr_2O_3$ ($0 \le x \le 20$ mole%) glass samples.

Wavenumber/cm^{-1}	Band assignments
~ 133	Presence of the Bi^{3+} cations as [BiO_6]
270–580	Bi–O–Bi angular vibrations belong to [BiO_6] polyhedra
~ 683	Stretching vibrations of B–O-bonds
~ 863	Symmetric stretching vibrations of B–O–B bridges
~ 1258	Vibrations of pyroborate groups
~ 1326	$B\O_2O^-$ triangles linked to $B\O_4^-$ units
~ 1400	Stretching of B–O bands attached to the borate groups

4. Conclusions

A qualitative investigation on $x$$CaF_2$–$(20-x)$$ZnF_2$–$20Bi_2O_3$–$59.8B_2O_3$–$0.2Cr_2O_3$ (x = 0, 5, 10, 15, and 20 mole%) glass samples has been undertaken to study the effect of metal fluorides using physical, optical, EPR, FTIR, and Raman studies. Glasses were prepared by using the melt quenching method and the amorphous nature of the glass samples was confirmed by XRD. The density of the glass decreases, which can be explained by the fact that the crystal density of calcium fluoride (3.18 gm/cc) is lower than zinc fluoride (4.95 gm/cc). The optical band gap (E_{opt}) for CZBBCR1 glass has a smaller value, but the addition of a small amount of CaF_2 increases the band gap. Thereafter, the band gap decreases with the increase in CaF_2 content. This variation is explained by using the ionicity of fluorine ions which increases with the increase of CaF_2. Relatively high refractive index in the present glasses can be used in many applications like fiber optic communication. Orderliness of glass structure increases with the increase in CaF_2, which is confirmed by the Urbach energy values. The lower values of B suggest that d-shell electrons of Cr^{3+} ions are shielded by boron network. The D_q values indicate that the Cr^{3+} ions are in strong crystal field. Two resonance signals near 4.2 (low field) and 1.97 (high field) have been observed in the EPR spectra, which are attributed to isolated ions of chromium and the exchange-coupled pairs Cr^{3+}–Cr^{3+}, respectively. The structural studies (FTIR and Raman) confirmed the presence of BO_3, BO_4, BiO_3, and BiO_6 units. Metal cation (Zn^{2+} and Ca^{2+}) units and Bi–O bond vibrations in BiO_3 units were also noticed.

References

[1] Chandra Sekhar K, Abdul Hameed, Sathe G, Narasimha Chary M and Shareefuddin Md 2018 *Bull. Mater. Sci.* **41** 79
[2] Yang J H, Dai S X and Wen L 2002 *Chin. Phys. Lett.* **19** 1516
[3] Xun D, Yang J, Xu S, Dai N, Wen L, Hu L and Jiang Z 2003 *Chin. Phys. Lett.* **20** 130
[4] Srinivas B, Abdul Hameed, Vijaya Kumar R, Narasimha Chary M and Shareefuddin Md 2018 *Phil. Mag.* **98** 1625
[5] Massot M, Souto S and Balkanski M 1995 *J. Non-Cryst. Solids* **182** 49
[6] Tian Y, Jing X and Xu S 2013 *Spectrochim. Acta Part. A* **115** 33
[7] Zheng T, Qin J M, Jiang D Y, Lü J W and Xiao S C 2012 *Chin. Phys. B* **21** 043302
[8] Chandra Sekhar K, Abdul Hameed, Ramadevudu G, Narasimha Chary M and Shareefuddin Md 2017 *Mod. Phys. Lett. B* **31** 1750180
[9] Tian Y, Jing X, Li B, Li P, Li Y, Lei R, Zhang J and Xu S 2016 *Opt. Mat. Exp.* **6** 3274
[10] Pisarska J, Zur L and Wojciech W A 2012 *Phys. Status Solidi A* **209** 1134
[11] Tian Y, Wei T, Jing X, Zhang J and Xu S 2016 *Mater. Res. Bull.* **76** 67
[12] Saddeek Yasser B, Essam Shaaban R, Sayed Moustafa El and Hesham Moustafa M 2008 *Phys. B* **403** 2399
[13] Shaaban E R, Shabaan M and Saddeek Y B 2008 *J. Phys. Conden. Matter* **20** 155108
[14] Punia R, Kundu R S, Hooda J, Dhankhar S, Dahiya S and Kishore N 2011 *J. Appl. Phys.* **110** 033527
[15] Saritha D, Markandeya Y, Salagram M, Vithal M, Singh A K and Bhikshamaiah G 2008 . *J. Non-Cryst. Solids* **354** 5573
[16] Kundu R S, Dhankhar S, Punia R, Nanda K and Kishore N 2014 *J. Alloy. Comp.* **587** 66
[17] Thakur V, Kushwaha H S, Singh A, Vaish R, Punia R and Singh L 2015 *J. Non-Cryst. Solids* **428** 197
[18] Lalitha Phani A V, Chandra Sekhar K, Chakradhar R P S, Narasimha Chary M and Shareefuddin Md 2018 *Mater. Res. Express* **5** 035204
[19] Stevenson A J, Serier-Brault H and Gredin P 2011 *J. Fluorine Chem.* **132** 1165

[20] Venkateswara Rao G and Shashikala H D 2014 *J. Adv. Ceram.* **3** 109
[21] Josse E, Fonteneau G and Lucas 1997 *J. Mater. Res. Bull.* **32** 1139
[22] Nazabal V, Poulain M and Olivier M 2012 *J. Fluorine Chem.* **134** 18
[23] Manoj Kumar N and Shashikala H D 2015 *J. Non-Cryst. Solids* **430** 79
[24] Djouama T, Boutarfaia A and Poulain M 2008 *J. Phys. Chem. Solids* **69** 2756
[25] Chandra Sekhar K, Abdul Hameed, Narasimha Chary M and Shareefuddin Md 2015 *AIP Conf. Proc.* **1665** 070030
[26] Duygu Aydın Y, Metin G, Dilek I and Dursun Ö 2017 *Arab J. Sci. Eng.* **42** 4409
[27] Sands R H 1955 *Phys. Rev. B* **99** 1222
[28] Wong J and Anjell C A 1976 *Glass Structure by Spectroscopy* (New York: Dekker)
[29] Padlyak B V, Ryba-Romanowski W, Lisiecki R, Adamiv V T, Burak Ya V and Teslyuk I M 2012 *Opt. Mater.* **34** 2112
[30] Samdani, Ramadevudu G, Narasimha Chary M and Shareefuddin Md 2017 *Mater. Chem. Phys.* **186** 382
[31] Lesniewski T, Padlyak B V, Barzowska J, Mahlik S, Adamiv V T, Nurgul Z and Grinberg M 2016 *Opt. Mater.* **59** 120
[32] Bala Murali Krishna S, Vinaya Teja P M and Krishna Rao D 2010 *Mater. Res. Bull.* **45** 1783
[33] Hassan M A 2013 *J. Alloy. Comps.* **574** 391
[34] Chandra Sekhar K, Srinivas B, Narsimlu N, Narasimha Chary M and Shareefuddin Md 2017 *Mater. Res. Express* **4** 105203
[35] Saddeek B Y, Aly A K and Bashier A S 2010 *Physica B* **405** 2407
[36] Doweidar H and Saddeek Y B 2009 *J. Non-Cryst. Solids* **355** 348
[37] Mohamed Raheem A, Chandra Sekhar K, Abdul Hameed, Narasimha Chary M and Shareefuddin Md 2018 *Int. J. Mod. Phys. B* **32** 1850095
[38] Sindhu S, Sanghi S, Agarwal A, Seth V P and Kishore N 2005 *Phys. B* **365** 65
[39] Doweidar H, Megahed A and Gohar I A 1986 *J. Phys. D* **19** 1939
[40] Watanabe H 1966 *Operator Methods in Ligand Field Theory* (Englewood Cliffs, NJ: Prentice-Hall)
[41] Tanabe Y and Sugano S 1954 *J. Phys. Soc. Jpn.* **9** 753
[42] Rasheed F, Donnel K P O, Henderson B and Hollis D B 1991 *J. Phys. Condens. Matter* **3** 1915
[43] Kesavulu C R, Chakradhar R P S, Muralidhara R S, Rao J L and Anavekar R V 2010 *J. All. Comps.* **496** 75
[44] Long X, Lin Z, Hu Z, Wang G and Han T P J 2002 *J. Alloys Compd.* **347** 52
[45] Davis A and Mott N F 1970 *Phil. Mag.* **22** 903
[46] Tauc J and Menth A 1972 *J. Non-Cryst. Solids* **8** 569
[47] Hasan M A and Hogarth C A 1988 *J. Mater. Sci.* **23** 2500
[48] Dahiya M S, Khasa S and Agarwal A 2015 *J. Asi. Ceram. Societies* **3** 206
[49] Dimitrov V and Sakka S 1996 *J. Appl. Phys.* **79** 1736
[50] Dimitrov V and Komatshu T 2002 *J. Solid State Chem.* **163** 100
[51] Rama Sundari G, Pushpa Manjari V, Raghavendra Rao T, Satish D V, Rama Krishna Ch, Venkata Reddy Ch and Ravikumar R V S S N 2014 *Opt. Mater.* **36** 1329
[52] Legein C, Buzar J, Emery J and Jacoboni C 1995 *J. Phys.: Condens. Mater.* **7** 3853
[53] Yusub S and Krishna Rao D 2014 *J. Non-Cryst. Solids* **398** 1
[54] Santhan Kumar J, Lakshmi Kumari J, Subba Rao M and Sandhya C 2013 *Opt. Mater.* **35** 1320
[55] De F S, Santos F A, Simões B S, Dias S T and Siu Li M 2014 *Opt. Mater.* **38** 119
[56] Weil J S and Bolton J R 2007 *Electron Paramagnetic Resonance Elementary Theory and Practical Applications*, Vol. 194 (New York: John Wiley) p. 498
[57] Aschcroft N W and Mermin N D 2001 *Solid State Physics* (Harcourt College Publishers) p. 656
[58] Kamitsos E, Karakassides M and Chryssikos G 1987 *J. Phys. Chem.* **91** 1073
[59] Yiannopoulos Y D, Chryssikos G D and Kamitsos E I 2001 *Phys. Chem. Glasses* **42** 164
[60] Kumar A, Rai S B and Rai D K 2003 *Mater. Res. Bull.* **38** 333
[61] Sumalatha B, Omkaram I, Rajavardhana Rao T and Linga Raju Ch 2013 *Phys. B* **411** 99
[62] Girsova M, Goloina G, Kuilenko L and Antropova T 2015 *Glass. Phy. Chem.* **41** 93
[63] El Batal F H 2007 *Nucl. Instrum. Methods Phys. Res. Sect. B: Beam Interact. Mater. Atoms* **254** 243
[64] Chandrakiram G, Kumar Yadav A and Kumar Singh A 2012 *ISRN Ceram.* 428497
[65] Rada S, Ristoiu T, Rada M, Coroiu I, Maties V and Culea E 2010 *Mater. Res. Bull.* **45** 69
[66] Balachander L, Ramadevudu G, Shareefuddin Md, Sayanna R and Venudhar Y C 2013 *Sci. Asia* **39** 278
[67] Lucian B, Razvan S, J€urgen P, Simion S and Wolfgang K 2003 *J. Non-Cryst. Solids* **324** 109
[68] Kharlamov A A, Almeida R M and Heo J 1996 *J. Non-Cryst. Solids* **202** 233
[69] Subhadra M and Kistaiah P 2012 *Vib. Spect.* **62** 23
[70] Kamitsos E I, Karakassides M A and Cryssikos G D 1987 *J. Phys. Chem.* **91** 1073
[71] Naresh V and Buddhudu S 2012 *Ceram. Inter.* **38** 2325